

Semi-mechanistic Modeling of an Osmotic Dehydration Process.

CARLOS COLLAZOS

Universidad Manuela Beltrán
Av. Circunvalar No 60-00, Bogotá
COLOMBIA
carlos.collazos@docentes.umb.edu.co

JORGE CARDONA

Universidad Manuela Beltrán
Av. Circunvalar No 60-00, Bogotá
COLOMBIA
jorge.cardona@docentes.umb.edu.co

HERMES CASTELLANOS

Universidad Manuela Beltrán
Av. Circunvalar No 60-00, Bogotá
COLOMBIA

hermes.castellanos@umb.edu.co

JAVIER CUERVO

Universidad Nacional de Colombia
Carrera 45 No 26-85, Bogotá
COLOMBIA

jacuervo@unal.edu.co

ARY BURBANO

Universidad Manuela Beltrán
Av. Circunvalar No 60-00, Bogotá
COLOMBIA

ary.burbano@docentes.umb.edu.co

ADRIANA MALDONADO

Universidad Nacional de Colombia
Carrera 45 No 26-85, Bogotá
COLOMBIA

amaldonadof@unal.edu.co

Abstract: This article presents a semi-mechanistic model (a hybrid of the classic and fuzzy models) of an osmotic dehydration process of pineapple. The fuzzy model (Takagi-Sugeno) represents a kinetic parameter of the physical process and it is developed through fuzzy classification of data (Gustaffson-Kessel algorithm). The fuzzy model is then incorporated in the mass conservation equation (classic model) aiming at the numerical prediction of the process. Experiments and validations are presented.

Key-Words: Physics Model, Osmotic Dehydration

1 Introduction

Physical modeling is fundamental for analysis, design, control and optimization of processes in science and engineering. A physical model is useful as it resembles the behavior of a process in a determined operation zone.

In complex systems, such as the processes that are carried out on an industrial level, physical modeling can be approached through two methodologies. The first is the classical modeling methodology and it focuses the study of the process on the fundamental principles of physics such as the mass, energy and moment conservation theorems. Mathematically, this kind of model is represented through difference equations, which are defined using state variables, constants and parameters.

When formalizing real systems, the relationship between inputs and outputs is described qualitatively, in the form of statements by production regulations. Fuzzy models have been proved to be good in several different applications [1], [2], [3], [4]. Particularly, fuzzy modeling has successfully been used in many cases of intelligent control [5],[6]. In this methodology, the identification of the parameters is done by using soft-computing techniques (which include fuzzy models, neural networks and adaptive network-based fuzzy inference system or ANFIS). ANFIS has proven a growing use in representing physical, chemical and biochemical processes, where partially known expressions exist, such as kinetic parameters, which involve

the handling of highly empiric models that are valid only for certain conditions or circumstances in the process. As an application of the semi-mechanistic model, the osmotic dehydration of pineapple process has been modeled combining these two methods.

The article is organized as follows. Section 2 describes the studied process and the experimental conditions of the process, the experiments and the dehydration plant. Section 3 presents the classical model. Section 4 reviews the fundamental concepts of fuzzy classification, identification and modeling techniques. Section 5 poses the semi-mechanistic model. Section 6 compares the results of the semi-mechanistic and classic models. Section 7 concludes the article, explaining the importance of the obtained results.

2 Process Description

2.1 Generalities

Osmotic dehydration is defined as a process where two phenomena are combined (dehydration and osmosis) and occur through a semi-permeable membrane: the cell wall [7],[8].

Pineapple is a completely heterogeneous, highly watery and porous food, that when submerged in solutions with high concentration of soluble solids (sugar), provokes two simultaneous upstream main flows (Figure 1) [9],[10]:

1. Transfer of soluble solids (sugar) from the solu-

tion to the food.

2. Flow of water from the food to the solution.

A third secondary and negligible flow of aroma, vitamins and minerals happens, which is less intense, and occurs from the fruit to the solution.

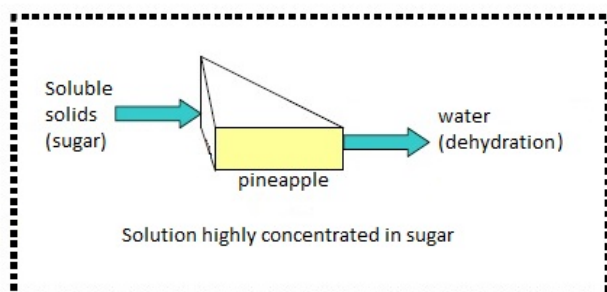


Figure 1: Mass transfer process between solution and food

The mass transfer mechanisms that are present in the osmotic dehydration at atmospheric pressure and room temperature are mainly diffusion (Fick's laws of diffusion). These mechanisms are originated by the concentration differences between the food and the osmotic solution [8], [11].

The sugar concentrations found in the osmotic solution and the food (mechanically extracted juice of the pineapple sample) are obtained for each sample time, ΔT . These measurements are registered by refractometers and reported in refraction indexes or Degrees Brix. Degrees Brix can be understood as a percentage from 0 to 1 or a mass fraction, that provides the sugar mass contained in the mass of each analyzed component (solution and biomass). When dehydration occurs, changes happen in the composition of the food and the osmotic solution. These changes have been analyzed in terms of mass balances for sugar gain $[X^S]$ and loss $[Y^S]$.

2.2 Plant Description

A typical profile of the previous variables for the process in Batch regime is indicated in [9], [11], [12] and [13]. The plant has worked in Fed-Batch regime (Figure 2). A secondary tank (tank 2) has been used, with a high concentration in sugar $[Y^S]_{cte} = 0.65$ Degrees Brix and initial volume of $[V]_1 = 40$ liters, to feed the main tank (tank 1, the reactor where the fruit dehydration process takes place), aiming at maintaining its sugar concentration above an initial and reference value $[Y^S]_{ref} = 0.6$ Degrees Brix.

This article is limited to Fed-Batch regime experiments because of the transcendence it has on the process control and optimization, since maintaining the

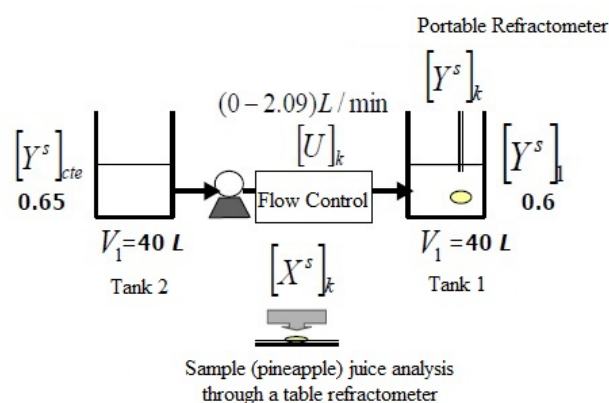


Figure 2: Dehydration plant diagram, Unitary Operations Lab., Engineering School, Universidad de La Sabana, Colombia

fruit under high concentration conditions, generates better results in the dehydration.

2.3 Experimental conditions and experiments

The used raw material was pineapple (*ananas comosus* in the cayena lisa variety) in a geometric shape (eighths of slice of 1 cm of thickness without any previous treatment).

The attributes of the osmotic solution for each tank were:

- Tank 2: Constant. $[Y^S]_{cte} = 0.65$ Degrees Brix. This is obtained by mixing approximately 61.5 kg of sugar with 40 kg of water.
- Tank 1: Reference. $[Y^S]_{ref} = 0.6$ Degrees Brix. This is obtained by mixing approximately 83.3 kg of sugar with 50 kg of water.

The plant was operating for two Fed-Batch regime experiments:

- Experiment 1: Ascending linear entry flow. $[U_1] =$ From 0 to 2.09 L/min in 180 minutes.
- Experiment 2: Constant linear entry flow. $[U_2] =$ 0.44 L/min for 180 minutes.

3 Classic Model

The dynamic process is discrete, with a sampling time of ΔT , which is practically the time that the fruit spends submerged in the solution. For this time, the available information is the flow entering tank 1, $[U]_k$, and the sugar concentrations are being measured simultaneously in the food, $[X^S]_k$, and in the solution, $[Y^S]_k$, (Figure 2).

Based on multiple investigations developed around the kinematics of the dehydration process, [9], [11], [12], [14], the classic model, in terms of mass balance carried away in a fixed time interval, is formulated in difference equations and represented as follows:

- Variation of sugar concentration for the solution:

$$[Y^S]_{k+1} = [Y^S]_k - B[C]_k[X^S]_k\Delta T + ([Y^S]_{cte} - [Y^S]_k)\frac{[U]_k\Delta T}{[V]_k} \quad (1)$$

- Variation of sugar concentration for the food:

$$[X^S]_{k+1} = [C]_k[X^S]_k\Delta T + \frac{[U]_k[X^S]_k\Delta T}{[V]_k} \quad (2)$$

Where:

- $[V]_k$ is the variation of tank 1 volume:

$$[V]_{k+1} = [V]_k + [U]_k\Delta T \quad (3)$$

- $[C]_k$ is the specific rate of sugar concentration in food:

$$[C]_k = \mu \frac{[Y^S]_k}{K_{Y^S} + [Y^S]_k} \quad (4)$$

- B is a dimensionless proportion factor between the concentration variation of the food and that of the solution. It is calculated using the final (subindex f) and initial (subindex o) values of the concentrations in solution and food:

$$B = \frac{[Y^S]_f - [Y^S]_o}{[X^S]_f - [X^S]_o} \quad (5)$$

- μ is the maximum change rate in sugar growth for the food. It is calculated using the final (subindex f) and initial (subindex o) values of the concentrations in food and the experimentation time. It is represented by:

$$\mu = \frac{\ln\left(\frac{[X^S]_f}{[X^S]_o}\right)}{t_f - t_o} \quad (6)$$

- $K_{Y^S} = 0.65$ (gr. of sugar/ gr. of osmotic solution in tank 1) is the saturation constant for sugar concentration in tank 1.

3.1 Calculations for kinetic parameter and constants

The calculation of the kinetic parameter $[C]_k$ and the kinetic constants μ and B is empirically done with the data and the equations 5 and 6 respectively.

Table 1 shows the results of the calculations for experiments 1 and 2.

Table 1: Kinetic constants for experiments 1 and 2

Experiment	μ L/min	B
Experiment 1	0.0008	0.51
Experiment 2	0.0007	0.27

Figures 3 and 4 present the experimental data and the weighing of $[C]_k$ using the information in table 1 and equation 4.

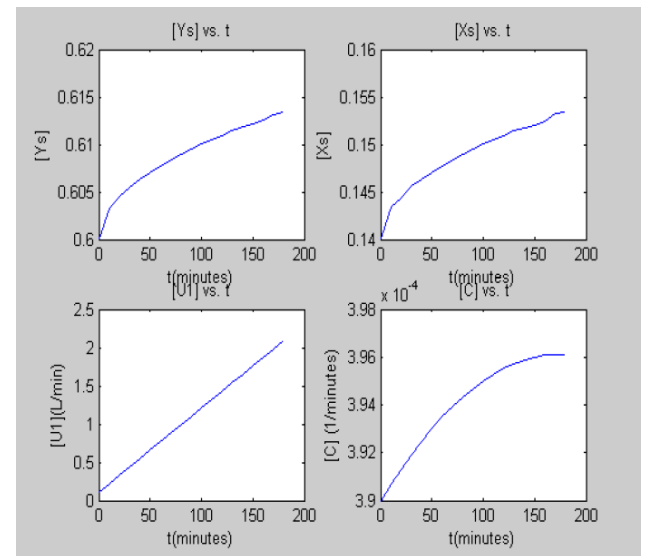


Figure 3: Experimental data and calculation of $[C]_k$ for the classic model, in experiment 1

3.2 Nomenclature

- ΔT : sample time (10 minutes)
- $(t_f - t_o)$: experimentation time (180 minutes)
- $[V]$: variable volume in tank 1 (liters)
- $[V]_1$: initial volume in tank 1 and tank 2 (40 liters)
- $[U]$: entry flow tank 1 (L/min)
- $[U_1]$: entry flow to tank 1 (L/min) in experiment 1
- $[U_2]$: entry flow to tank 1 (L/min) in experiment 2
- $[X^S]$: mass fraction of soluble solids (sugar) in food
- $[Y^S]$: mass fraction of soluble solids (sugar) in solution tank 1
- Degrees Brix* (gr. sugar/ gr. osmotic solution tank 1)

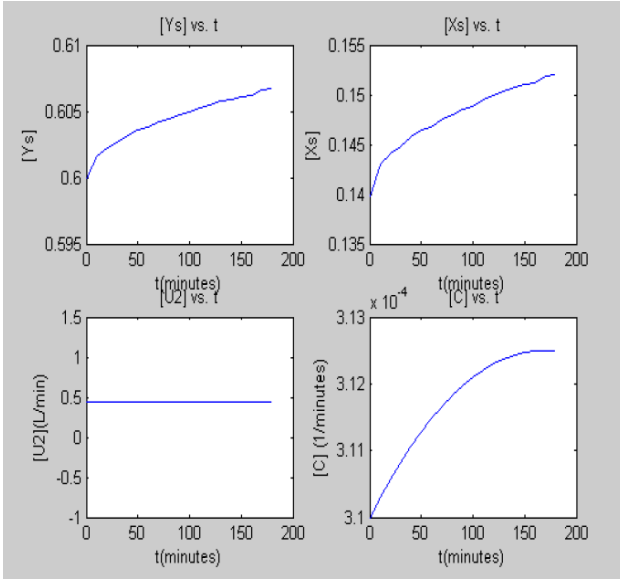


Figure 4: Experimental data and calculation of $[C]_k$ for the classic model, in experiment 2

$[Y^S]_{cte} = 0.65$: mass fraction of soluble solids (sugar) in solution tank 2 Degrees Brix (gr. sugar/ gr. osmotic solution tank 2)

$[C]$: specific rate of soluble solids (sugar) concentration for food (L/min)

B : proportion factor (dimentionless)

$K_{Ys} = 0.65$: saturation constant for soluble solids (sugar) concentration in tank 1 (gr. sugar/ gr. osmotic solution tank 1)

μ : maximum change rate in soluble solids (sugar) growth for food (L/min)

k : discrete time

4 Fuzzy Logic Principles

Within the fuzzy scope, models are defined through membership functions and rules, which are found using the system's input and output data with classification algorithms.

4.1 Takagi-Sugeno Model (T-S)

The T-S model is a fuzzy model made of R_i rules, like follows [14], [15], [16], [17], [18], [19]:

R_i : if x is A_i , then

$$Y_i = \mathbf{a}_i^T x + b_i; \quad i = 1, 2, \dots, k \quad (7)$$

Where x is the input vector, A_i is the fuzzy set (multidimensional), Y_i is the output of the i -th rule, \mathbf{a}_i is a parametric vector and b_i is the scalar displacement, namely, the antecedent is calculated through

fuzzy rules, while the consequent is a linear combination of the variables of the antecedent. Therefore, the inputs x , that are A_i , are represented as a combination of monodimensional propositions defined by each component of the input vector x .

R_i : if x_1 is A_{i1} and ... and x_p is A_{ip} then

$$Y_i = \mathbf{a}_i^T x + b_i; \quad i = 1, 2, \dots, k \quad (8)$$

In the i -th rule, the p variables x_1, \dots, x_p that form the antecedent are related to fuzzy sets A_1, \dots, A_p , while Y_i is a function where the antecedent variables participate. The previous characteristic allows its application in static and dynamic MIMO systems (multi-input/multi-output).

The global output of the model is obtained by adding rules and defuzzification, according to traditional methods. To determine the inference of the T-S model, first, it is necessary to take into account the degree of fulfillment of the antecedent $\beta_i(x)$, which is calculated as the membership degree of x in the fuzzy set A_i : $\beta_i = \mu_{A_i}(x)$. For rules with fuzzy MIMO sets, the fulfillment degree of the antecedent is calculated through combinations of membership degrees of the individual propositions using logic connectives, like the T-norm, where the fulfillment degree $\beta_i(x)$ is calculated as:

$$\beta_i(\mathbf{x}) = \mu_{A_{i,1}}(x_1) \wedge \mu_{A_{i,2}}(x_2) \wedge \dots \wedge \mu_{A_{i,p}}(x_p) \quad (9)$$

For the individual outputs of the consequent Y_i , the global output of the fuzzy T-S model, with N rules is calculated using the weighted average formula. In that case, the inference is reduced to:

$$Y = \frac{\sum_{i=1}^N \beta_i(\mathbf{x}) y_i}{\sum_{i=1}^N \beta_i(\mathbf{x})} \quad (10)$$

The T-S model is expressed as a pseudolinear model with parameters that depend on the inputs:

$$y = \left(\sum_{i=1}^R \lambda_i(\mathbf{x}) \mathbf{a}_i^T \right) \mathbf{x} + \sum_{i=1}^R \lambda_i(\mathbf{x}) b_i = \mathbf{a}^T(\mathbf{x}) \mathbf{x} + b(\mathbf{x}) \quad (11)$$

The parameters $\mathbf{a}(\mathbf{x})$ and $b(\mathbf{x})$ are convex linear combinations of the parameters of the consequent \mathbf{a}_i and b_i , namely:

$$\mathbf{a}(\mathbf{x}) = \sum_{i=1}^N \lambda_i(\mathbf{x}) \mathbf{a}_i \quad (12)$$

$$b(\mathbf{x}) = \sum_{i=1}^N \lambda_i(\mathbf{x}) b_i \quad (13)$$

The previous terms show that T-S models can play the role of function regressors, namely, they approximate, with good exactitude, a function $y = f(x)$.

4.2 Gustafson-Kessel Algorithm (G-K), based on C-means

The classification techniques seek to find subsets with certain degree of similitude within a set of data, whether it is on a quantitative level or qualitatively. The data are observations of a process (physical, chemical, etc.). Each observation consists of n measured variables, expressed in an n -dimensional column $z_k = [z_{1k}, \dots, z_{nk}]^T, z_k \in \mathbb{R}^n$. A set of N observations is denoted by $\{Z_k \mid k = 1, 2, \dots, N\}$ and it is represented as a $n \times N$ matrix:

$$Z = \begin{bmatrix} z_{11} & z_{12} & \dots & z_{1N} \\ z_{21} & z_{22} & \dots & z_{2N} \\ \vdots & \vdots & \ddots & \vdots \\ z_{n1} & z_{n2} & \dots & z_{nN} \end{bmatrix} \quad (14)$$

Before reviewing the classification techniques, it is convenient to define a *cluster* as a group of objects that are more similar among them than other members of other groups [14]. The concept of "similarity" can be understood as a mathematical likeness, measured in metric spaces and defined through a distance norm. The distance can be measured between the same data vectors or as a distance from one data vector to some prototypical object (centers) of the cluster [15].

One of the first proposed classification techniques that uses objective function optimization is C-means by Bezdek in 1981. The similarity measurement of this technique is capable of detecting a cluster in a circular shape. Gustaffson and Kessel extended the C-means algorithm by using an adaptative distance norm for differently shaped cluster location effects in the set of data. Each cluster has its own induced norm matrix, A_i , which originates the norm of the internal product [16]:

$$D_{ikA_i}^2 = (\mathbf{z}_k - \mathbf{v}_i)^T \mathbf{A}_i (\mathbf{z}_k - \mathbf{v}_i) \quad (15)$$

The matrices A_i are used as optimization variables in the functional of C-means,

$$J(\mathbf{Z}; \mathbf{U}, \mathbf{V}) = \sum_{i=1}^c \sum_{k=1}^N (\mu_{ik})^m \| \mathbf{z}_k - \mathbf{v}_i \|_{A_i}^2 \quad (16)$$

where:

$$\mathbf{U} = [\mu_{ik}] \in \mathbf{M}_{fc} \quad (17)$$

\mathbf{U} is a fuzzy partition matrix of \mathbf{Z} , that belongs to the fuzzy partition matrix space, \mathbf{M}_{fc} and contains all the values of the membership functions of each object to each of the prototype centers c , where \mathbf{V} is the vector of prototypes of cluster (centers) [17]

$$\mathbf{V} = [\mathbf{v}_1, \mathbf{v}_2, \dots, \mathbf{v}_c], \mathbf{v}_i \in \mathbb{R}^n \quad (18)$$

This way, each cluster adapts its distance norm to the local data structure. To obtain a feasible solution, \mathbf{A}_i must be limited, which is achieved by allowing a variation in the form of the cluster and keeping its volume ρ_i constant [8]:

$$|\mathbf{A}_i| = \rho_i, \rho_i > 0, \forall i \quad (19)$$

Using Lagrange multipliers' method, \mathbf{A}_i is obtained:

$$\mathbf{A}_i = [\rho_i \det(\mathbf{F}_i)]^{1/n} \mathbf{F}_i^{-1} \quad (20)$$

Where \mathbf{F}_i is the fuzzy covariance matrix of the i -th cluster, defined by:

$$\mathbf{F}_i = \frac{\sum_{k=1}^N (\mu_{ik})^m (\mathbf{z}_k - \mathbf{v}_i)(\mathbf{z}_k - \mathbf{v}_i)^T}{\sum_{k=1}^N (\mu_{ik})^m} \quad (21)$$

4.3 Building fuzzy T-S models from partitions

The clusters obtained by data classification are a local linear approximation of the regression hypersurface. The whole of the global model can be represented by a T-S model. Then each cluster is converted into a T-S rule, defined by parameters of the consequent and the membership functions of the antecedent, that are obtained from the fuzzy partition matrix [14], [15].

5 Physical model: a hybrid of the classic and fuzzy models

A block representation of the semi-mechanistic model, using a white-box (classic model) and black-box (Takagi-Sugeno fuzzy model) is presented in figure 5. The white box is directly associated to the balance and flow equations 1, 2, 3, defined in section 3. The black box is originated by previously defining an unknown dependency between $[C]_k$ with $[X^S]_k$ and $[Y^S]_k$, which is represented in the form:

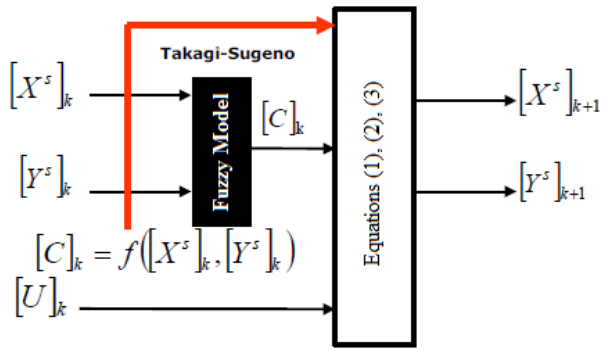


Figure 5: Semi-mechanistic model structure. The red arrow represents the concentrations $[X^S]_k, [Y^S]_k$ as inputs of the classic model

$$[C]_k = f([X^S]_k, [Y^S]_k) \quad (22)$$

This dependence in modeling terms could be represented as a fuzzy model (black-box) with 2 inputs: $[X^S]_k$ and $[Y^S]_k$ and an output: $[C]_k$. The purpose of this methodology is precisely to define the unknown dependency $f(\cdot)$ from a Takagi-Sugeno fuzzy model. The previously defined fuzzy model is used as a numeric predictor of $[C]_k$ and the obtained prediction is explicitly replaced in equations 1 and 2 of the classic (white-box) model. To determine the T-S model, the Gustafson-Kessel algorithm was used and the experimental data which was organized in a data matrix \mathbf{Z} like follows:

$$\mathbf{Z}^T = \begin{bmatrix} [Y^S]_1 & [X^S]_1 & [C]_1 \\ \vdots & \vdots & \vdots \\ [Y^S]_n & [X^S]_n & [C]_n \end{bmatrix} \quad (23)$$

In the validation of the T-S model, the data of section 3 was used. Meanwhile, the identification was done with different experimental data than those used in the validation, but taken under the same experimental conditions, which allowed the *a-posteriori* estimation of $[C]_k$. The previously exposed methodology allows making comparisons between the classic and the semi-mechanistic models from the two interpretations available to define $[C]_k$ for each case.

5.1 Calculation of the $[C]_k$ parameter through a T-S model

In the following graphs, the obtained T-S models for predicting $[C]_k$ in experiments 1 and 2. In the model estimation process, three clusters were used, which allowed the definition of the three rules and six membership functions (figures 7, 8, 9, 10). These results have

been obtained using the Babuska fuzzy modeling and identification toolbox [19].

The validation of the models was done through the root-mean-squared deviation (RMSD):

$$E_{RMSD} = \sqrt{\frac{\sum_{j=1}^N (y_j - \hat{y}_j)^2}{N}} \quad (24)$$

which depends on the number of used data, N , the experimental output, y_j , and the output forecast calculated by the T-S fuzzy model, \hat{y}_j . The validation of the model is indicated in figure 6.

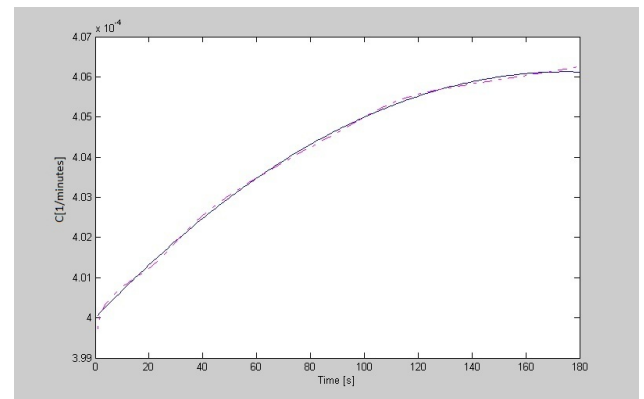


Figure 6: Validation of the T-S model that defines $[C]_k$ for the semi-mechanistic model, experiment 1. Purple line: output forecast by T-S model. Blue line: experimental $[C]_k$ output. $E_{RMSD} = 0.00021$.

5.2 Results for experiment 1

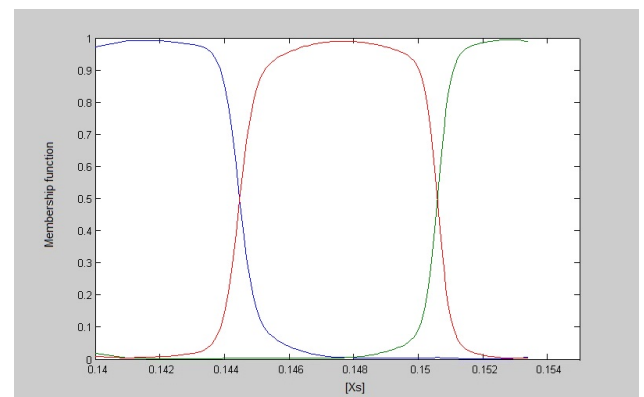


Figure 7: Membership functions $[X^S]$ of the T-S model for the $[C]_k$ forecast in the semi-mechanistic model, obtained by G-K algorithm, experiment 1.

The obtained rules from the T-S model for the $[C]_k$ forecast in the semi-mechanistic model for experiment 1 were:

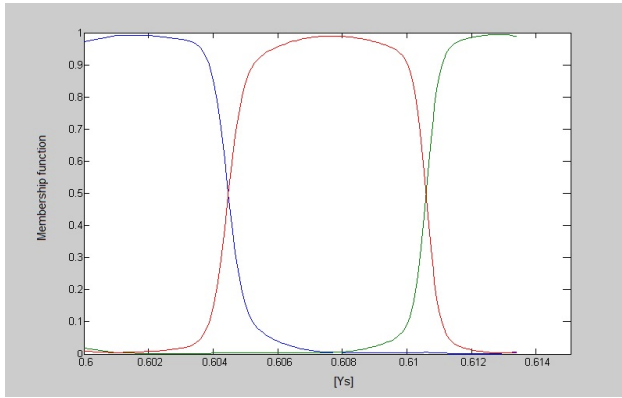


Figure 8: Membership functions $[Y^S]$ of the T-S model for the $[C]_k$ forecast in the semi-mechanistic model, obtained by G-K algorithm, experiment 1.

1. **If $[X^S]$ is A_{11} and $[Y^S]$ is A_{12} then**
 $[C] = 3.50 \times 10^{-3}[X^S] - 3.18 \times 10^{-3}[Y^S] + 1.82 \times 10^{-3}$
2. **If $[X^S]$ is A_{21} and $[Y^S]$ is A_{22} then**
 $[C] = 7.70 \times 10^{-4}[X^S] - 1.46 \times 10^{-4}[Y^S] + 3.78 \times 10^{-4}$
3. **If $[X^S]$ is A_{31} and $[Y^S]$ is A_{32} then**
 $[C] = 3.01 \times 10^{-3}[X^S] - 2.75 \times 10^{-3}[Y^S] + 1.63 \times 10^{-3}$

5.3 Results for experiment 2

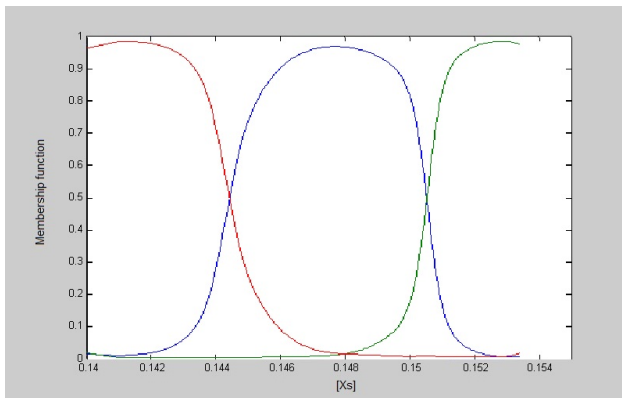


Figure 9: Membership functions $[X^S]$ of the T-S model for the $[C]_k$ forecast in the semi-mechanistic model, obtained by G-K algorithm, experiment 2.

The obtained rules from the T-S model for the $[C]_k$ forecast in the semi-mechanistic model for experiment 2 were:

1. **If $[X^S]$ is A_{11} and $[Y^S]$ is A_{12} then**
 $[C] = 3.05 \times 10^{-4}[X^S] - 2.97 \times 10^{-4}[Y^S] + 4.57 \times 10^{-4}$
2. **If $[X^S]$ is A_{21} and $[Y^S]$ is A_{22} then**
 $[C] = 2.21 \times 10^{-4}[X^S] + 1.21 \times 10^{-4}[Y^S] + 2.12 \times 10^{-4}$

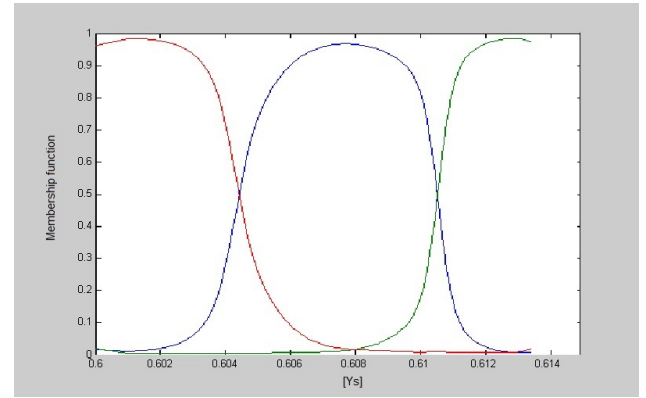


Figure 10: Membership functions $[Y^S]$ of the T-S model for the $[C]_k$ forecast in the semi-mechanistic model, obtained by G-K algorithm, experiment 2.

3. **If $[X^S]$ is A_{31} and $[Y^S]$ is A_{32} then**
 $[C] = 2.17 \times 10^{-4}[X^S] - 2.25 \times 10^{-4}[Y^S] + 4.21 \times 10^{-3}$

Table 2 presents the validations of the T-S models that forecast $[C]_k$ for experiments 1 and 2, based on equation 24 and the data used in figures 7 and 9.

Table 2: Validation of T-S models that predict $[C]_k$ for experiments 1 and 2.

E1 (eq. 24)	Exp. 1	Exp. 2
E1-[C]	0.00021	0.00022

Based on the validation process of the previously exposed T-S models, it can be stated that they make a very efficient estimation.

6 Results

Through the methodologies used to determine $[C]_k$, developed in sections 3 and 5, for the classic and semi-mechanistic models, their respective structures were used to generate, in a recurrent numerical fashion and from the initial conditions of the process, the prediction of the sugar concentration variations in food $[X^S]_{k+1}$ and the osmotic solution $[Y^S]_{k+1}$ for each flow input $[U]_k$ depending on the experiment. For this, an .m file was developed in Matlab[®], which loads the input data for both models, compiles the predictions and calculates the root-mean-squared deviation between the predictions and the experimental data. For the model validation, the RMSD equation has been re-interpreted, which is defined by equation 24, where N is the number of used data, y_j is the experimental data and \hat{y}_j is the estimated output of the classic and

semi-mechanistic models in each of the state variables $[X^S]$ and $[Y^S]$. As a comparison, figure 11 shows the prediction for the classic and semi-mechanistic models plus the experimental data in experiment 1. For experiment 2, the comparison of the models is shown in figure 12. Table 3 presents the validations of experiment 1, based on equation 24 and the information available in figure 11. Table 4 presents validations of experiment 2, based on equation 24 and the information available in figure 12.

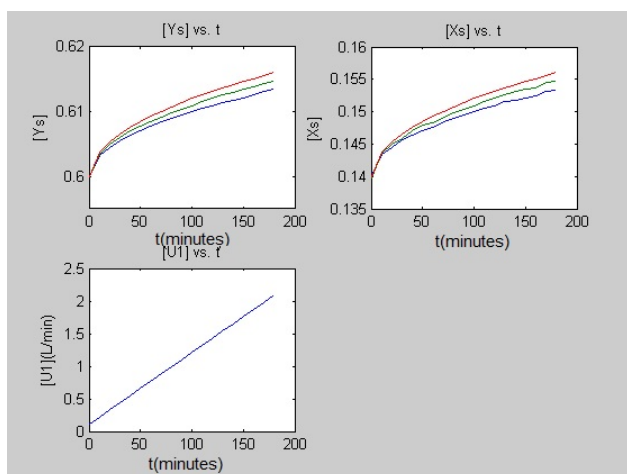


Figure 11: Comparison of model predictions and experimental data for experiment 1. Blue: experimental data. Red: Classic model. Green: Semi-mechanistic model.

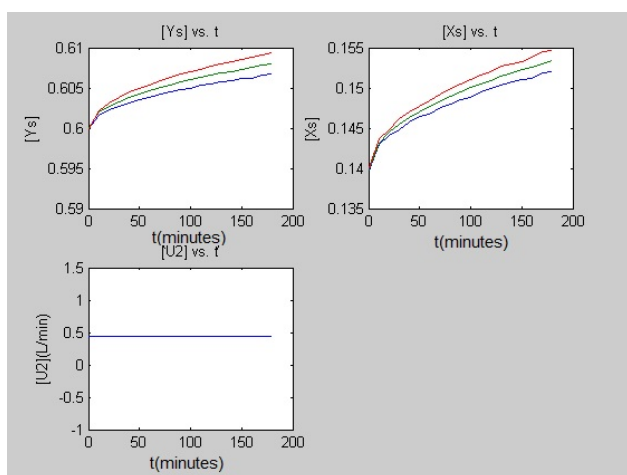


Figure 12: Comparison of model predictions and experimental data for experiment 2. Blue: experimental data. Red: Classic model. Green: Semi-mechanistic model.

After the validation process of these previously explained models, it can be concluded that they have

Table 3: Validation of classic and semi-mechanistic models for experiment 1.

E1 (eq. 24)	Classic model	Semi-mech. model
$E1 - [X^S]$	0.006248	0.003073
$E1 - [Y^S]$	0.006446	0.003165

Table 4: Validation of classic and semi-mechanistic models for experiment 2.

E1 (eq. 24)	Classic model	Semi-mech. model
$E1 - [X^S]$	0.006161	0.003165
$E1 - [Y^S]$	0.006349	0.003175

an acceptable performance in predicting the behavior of the analyzed osmotic dehydration process.

7 Conclusions

- The G-K classification and the fuzzy modeling and identification techniques given by R. Babuska's fuzzy modeling and identification toolbox are important tools that can be used as a complement of the numerical techniques of classical modeling to generate semi-mechanistic models.
- The recurring structure of the classic and semi-mechanistic models allows them to be used as numeric predictors of the process by defining the initial conditions of the process, the flow entry $[U]_k$ and the kinetic parameter $[C]_k$.
- The structures of the semi-mechanistic and classic models respectively, based on the approximation of $[C]_k$ through a model T-S technique and the calculation of $[C]_k$ through empirical methods in kinetics, may be used in the controller design field by using PID and non-linear control techniques.
- The obtained models open work perspectives around the interesting but not so trivial techniques of parametric optimization and identification.
- Agroindustrial and Food Production Engineering is another promising field where the automation

and control theory techniques can deepen in favor of obtaining high-quality food products for commercial and industrial ends.

References:

- [1] Z. Jiang and J. Zhang and M. Jin and B. Ma, An Expert system Based on Multi-Source Signal Integration for Reciprocating Compressor, *WSEAS Transactions on Systems*, Vol. 12, 2013, pp. 266-279.
- [2] S. Hrehova and A. Vagaska, Application of Fuzzy Principles in Evaluating Quality of Manufacturing Process, *WSEAS Transactions on Power Systems*, Vol. 7, 2012, pp. 50-59.
- [3] G. Wang and S. Chen and Z. Zhou and J. Liu, Modelling and Analyzing Trust Conformity in ECommerce Based on Fuzzy Logic, *WSEAS Transactions on Systems*, Vol. 14, 2015, pp. 1-10.
- [4] L. Borisova and I. Nurutdinova and V. Dimitrov, Fuzzy Logic Inference of Technological Parameters of the Combine-Harvester, *WSEAS Transactions on Systems*, Vol. 14, 2015, pp. 278-285.
- [5] A. M. Kassem, Fuzzy-Logic Based Self-tuning PI Controller for High-Performance Vector Controlled Induction Motor Fed by PVGenerator, *WSEAS Transactions on Systems*, vol. 12, pp. 22-31, 2013.
- [6] W. F. Xie and J. H. Ma, Optimization of a Vendor Managed Inventory Supply Chain Based on Complex Fuzzy Control Theory, *WSEAS Transactions on Systems*, vol. 13, pp. 429-439, 2014.
- [7] J.M. Barat, Desarrollo de un modelo de la deshidratación osmótica como operación básica. Doctoral Thesis. Universidad Politécnica de Valencia, Spain, 1990.
- [8] J. Crank, *The mathematics of the diffusion*, Lorendon Press, Oxford, U.K.,1975.
- [9] P. Fito and A. Chiralt, *Osmotic dehydration: An approach to the modeling of solid food-liquid operations*. *Food Engineering 2000*, Ed. Chapman & Hall, Spain, 2000, pp. 231-252.
- [10] G. González, Viabilidad de la piña colombiana var. cayena lisa para su industrialización combinando las operaciones de impregnación a vacío, deshidratación cayena lisa (*ananas comosus l. meer*) a través de un modelo matemático, Agroindustrial Engineering undergraduate thesis, Universidad de La Sabana, Colombia, 2000.
- [11] S. Jaller and S. Vargas, Comparación de la transferencia de materia en los procesos de deshidratación osmótica a presión atmosférica y con impregnación de vacío en la piña cayena lisa (*ananas comosus l. meer*) a través de un modelo matemático, Agroindustrial Engineering undergraduate thesis, Universidad de La Sabana, Colombia, 2000.
- [12] B. Wullner, Instrumentación y control de un deshidratador osmótico a vacío, Agroindustrial Engineering undergraduate thesis, Universidad de La Sabana, Colombia, 1998.
- [13] D. Torregiani, Osmotic dehydration of food, *Trends in Food Science & Technology*, Vol 5, 1995, p. 255-260.
- [14] T. Takagi and M. Sugeno, Fuzzy identification of systems and its applications to modeling and control, *IEEE Transactions Systems, Man, and Cybernetics*, 15, 116-132, 2011.
- [15] L. Wang, *A Course in Fuzzy Systems and Control*. Prentice Hall, 2007.
- [16] J. Abonyi and R. Babuska, Fuzzy Clustering for Identification of Takagi-Sugeno Fuzzy Models, *IEEE Trans. on Systems, Man and Cybernetic*, Part B, October, 2002.
- [17] R. Babuska, *Fuzzy Modeling for Control*, Kluwer Academic Publishers: Massachusetts, USA, 1998.
- [18] D. Gustafson and W. Kessel, Fuzzy Clustering with a Fuzzy Covariance, *Proc.IEEE CDC*, pp 761-766, San Diego, CA, USA, 1979.
- [19] R. Babuska, FAMIMO, <<http://www.iritidia.ulb.ac.be/FAMIMO>>, [cited on August 4th, 2015].